Local Density of States and Order Parameter Configurations in Layered Ferromagnet-Superconductor Structures.

Klaus Halterman

Sensor and Signal Sciences Division, Naval Air Warfare Center, China Lake, California 93555[1]

Oriol T. Valls

School of Physics and Astronomy and Minnesota Supercomputer Institute, University of Minnesota, Minneapolis, Minnesota 55455

Abstract

We analyze the local density of states (LDOS) of heterostructures consisting of alternating ferromagnet, F, and superconductor, S, layers. We consider structures of the SFS and $SFSFSFS$ type, with thin nanometer scale F and S layers, within the ballistic regime. The spin-splitting effects of the ferromagnet and the mutual coupling between the S regions, yield several nontrivial stable and metastable pair amplitude configurations, and we find that the details of the spatial behavior of the pair amplitude govern the calculated electronic spectra. These are reflected in discernible signatures of the LDOS. The roles that the magnetic exchange energy, interface scattering strength, and the Fermi wavevector mismatch each have on the LDOS for the different allowed junction configurations, are systematically investigated.

Key words: Proximity effect, Local DOS, Nanostructures, Superconductors, Magnets, Nanotechnology, π-junctions
PACS: 74.50+r, 74.25.Fy

Email addresses: klaus.halterman@navy.mil (Klaus Halterman), otvalls@umn.edu (Oriol T. Valls).

[1] This work was supported in part by a grant of HPC resources from the Arctic Region Supercomputing Center at the University of Alaska Fairbanks as part of the Department of Defense High Performance Computing Modernization Program.

1 Introduction

The continual investigation and development of heterostructures consisting of layered ferromagnet (F) and superconductor (S) compounds at nanometer length scales has captured the interest of researchers in a broad range of disciplines. The reasons for this stem from the distinctive properties of these nano-sized materials, modified from those of their bulk counterparts, related to the effects induced by the mutual coupling that occurs when superconductors and ferromagnets are in close electrical contact. The advancement of nanofabrication techniques is partly responsible for the maintained interest thus far, where electron-beam lithography, etching and lift-off methods, to name a few, have been refined to allow for the well controlled creation of relatively clean multiple layers involving F/S junctions. Further developments in experimental probes such as the scanning tunneling microscope (STM), have also progressed to the point where μeV energy resolution can be obtained at very low temperatures[1]. When operating in spectroscopy mode, the STM gives fine atomic-scale details of the local density of states (LDOS) of inhomogeneous superconducting systems. In contrast to conventional tunnel junctions, where transport measurements are taken, the STM gives localized spatial information not averaged out over the extent of the entire sample[2].

For composite materials comprised of multiple superconductor layers separated by ferromagnet materials, the presence of the magnetic F regions induces a splitting of the Fermi surfaces of the different spin bands, and leads to spin-dependent Andreev[3] states. The degree of spin-polarization in the superconductor and the induced pairing correlations in the ferromagnet are all components that embody what are known as proximity effects. It turns out that due to the mutual interaction between the two contrasting materials and the inherent system inhomogeneity, the pair amplitude, becomes spatially varying[4,5], and its phase difference $\Delta\phi$ can modulate between successive S layers. For certain configurations, there can be (at zero applied magnetic field) a phase difference of $\Delta\phi = \pi$ between S layers separated by a ferromagnet[6]. These are the so-called π junctions, which occur in the simplest case, in a 3-layer SFS type structure. Junctions of this type can also occur in different combinations for more complicated[7,8] layered heterostructures, where the relative sign of the pair potential $\Delta(\mathbf{r})$ can change between adjacent S layers. The proximity effect is then responsible for the existence of a number of stable junction configurations of the pair amplitude in F/S multilayers[9]: the oscillatory behavior of the superconducting correlations in each ferromagnet and the spatial profile of the pair amplitude in the superconductor are closely interconnected, often resulting in a nontrivial spatial dependence of the magnitude and phase of the order parameter. This consequently implies that the one-particle energy spectrum, or density of states (DOS), will have an equally interesting behavior.

The characteristic behavior of the DOS in structures consisting of a single ferromagnet and superconductor has been addressed in past work. In the diffusive, dirty-limit case, the damped-oscillatory decay of the pair amplitude in the F region induces a spatial variation of the LDOS[10]. For a clean F/S system with rough boundaries, the tunneling DOS as a function of energy revealed certain inversion signatures that depended on the thickness of the ferromagnet film [11]. The energy gap in F/S hybrid systems becomes rapidly suppressed, in a manner that depends on the ratio of the F and S Fermi energies, interfacial scattering strength, and F layer thickness[12]. The depletion of the gap has also been discussed in the context of a potential spin-valve device [13]. The spatially averaged DOS was calculated for a clean 2-D F/S box geometry[14], as was the LDOS for 3-D hybrid F/S nanostructures[15], where there was a reported filling in of the gap with increased F layer thickness. The damped oscillatory phenomena of the DOS is expected to persist over a broad range of material parameters [16]. For an SFS type structure, the proximity effect can lead to a modification of the LDOS that depends solely on the phase difference of the superconductors[17]. It was shown by using a two-band model for ferromagnetism, that the LDOS for a F/S bilayer still maintained the characteristic damped oscillations, with however, an increased wavelength and sharper decline [18]. Certain F/S bilayers with unconventional d-wave superconductors have also been investigated for peculiar characteristics of the DOS [19,20,21]. Thus, while the DOS and LDOS of F/S bilayers have been investigated, as have also to some extent SFS junctions, work analyzing the LDOS of junctions consisting of more than three layers is still scarce. It is imperative therefore to have a theory valid for these multilayers, since as potential device applications and experimental techniques become more advanced, the creation of complicated sequences of π-junctions will become increasingly realizable.

Much of the somewhat limited experimental work on the DOS in F/S heterostructures is based on transport measurements. Direct evidence of the oscillatory behavior of the superconducting correlations in the ferromagnet was found through tunneling spectroscopy measurements that showed inversions in the DOS for a thin ferromagnet film [22]. Modifications to the DOS in the superconductor also give insight in describing the proximity effect, by providing information on the influence of the ferromagnet on superconducting correlations. It was found that the DOS in the vicinity of the interface of the superconductor is substantially modified from the bulk BCS result[23]. Recently, local spectroscopy revealed the LDOS for a few different ferromagnet thicknesses [24]: the reported inversion of the DOS was attributed to the π state. Some other relevant experiments involving the ground state behavior of π-junctions have shown that both the 0 or π state can occur, depending on the width d_F of the F layer[25]. The origin of the damped oscillatory behavior reflected in DOS measurements and calculations discussed earlier is responsible, in some cases, for the damped oscillations in the critical current I_C as a

function of F layer width, suggesting a 0 to π transition[26]. The signature in the characteristic I_C curves also indicates a crossover from the 0 to π phase in going from higher to lower temperatures[27]. The current phase relation was also measured[28], demonstrating a re-entrant I_C with temperature variation.

Despite the existence of this experimental work, little attention has been paid until very recently to discussing, from a thermodynamic point of view, the relative stability of the different possible configurations involving 0 and π junctions in $SFS\ldots$ heterostructures. Indeed, a recent preprint[29] complains of the complete absence of work on thermodynamic properties of such structures. We have alleviated this situation in very recent work[9], where we have found a way to correctly evaluate the condensation free energy in these nanostructures as a function of the relevant parameters. The work that we discuss here involves discussing the LDOS for junction configurations whose thermodynamic stability properties are[9] well understood.

The quasiparticle amplitudes and energies that ultimately govern all observable behavior are very sensitive to the geometry of the given F/S system. For F or S layers a few nanometers thick, interference of the wavefunctions even over the atomic scale can produce significant contributions to the LDOS. Often the interaction potentials and geometry vary quite rapidly over the Fermi wavelength, and averaging over the momentum space trajectories eliminates useful information on the quasiparticle dynamics. It is therefore preferred in the clean limit situation considered here, to implement a microscopic model which affords the most complete information regarding the local electronic structure. This requires going beyond the standard approximate equations, e.g., the Eilenberger equations, which are essentially transport differential equations that describe superconductivity in the quasiclassical regime. With the progressive strides made in local spectroscopy techniques, a fully microscopic theory that allows inclusion of the details of the LDOS at the atomic scale is necessary. Furthermore the ground state properties of π junctions can be analyzed properly only if the superconducting order parameter is calculated self-consistently. The theory used here satisfies these requirements.

In this paper we calculate the LDOS for several possible multilayer structures. The existence of such structures as either local or global minima of the free energy was proved in Ref. [9]. Differing spectra are found depending on the exact nature of the particular junction configuration considered. By using an established fully microscopic method [7,30,31], we self-consistently calculate the pair potential, $\Delta(\mathbf{r})$, revealing several permissible types of spatial arrangements of the order parameter. The quasiparticle wavefunctions and associated energies are obtained from the microscopic Bogoliubov-de Gennes (BdG) equations. A numerical algorithm is then used that permits the self-consistent calculation of the pair potential. We find differing signatures for the LDOS that should be discernible in STM spectroscopy experiments.

2 Methods

In this section we outline the Bogoliubov-de Gennes (BdG) equations [32] that are appropriate for the investigations of F/S multilayered junctions. Since the BdG equations are inherently real-space based, they are especially convenient for the investigation of the possible spatial configurations of the pair amplitude and the spatially resolved LDOS.

We consider 3-D slab-like compounds translationally invariant in the $x-y$ plane, and with all spatial variations occurring in the z direction. The structures consists of alternating superconducting, S, and ferromagnetic, F, layers, each of width d_S and d_F respectively. We call d the total thickness of the slab. The corresponding coupled equations for the spin-up and spin-down quasiparticle amplitudes $(u_n^{\downarrow}, v_n^{\uparrow})$ are written,

$$[-\frac{1}{2m}\frac{\partial^2}{\partial z^2} + \varepsilon_\perp - E_F(z) + U(z) - h_0(z)]u_n^{\uparrow}(z) + \Delta(z)v_n^{\downarrow}(z) = \epsilon_n u_n^{\uparrow}(z) \tag{1a}$$

$$-[-\frac{1}{2m}\frac{\partial^2}{\partial z^2} + \varepsilon_\perp - E_F(z) + U(z) + h_0(z)]v_n^{\downarrow}(z) + \Delta(z)u_n^{\uparrow}(z) = \epsilon_n v_n^{\downarrow}(z), \tag{1b}$$

where $\varepsilon_\perp$ is the kinetic energy term corresponding to quasiparticles with momenta transverse to the z direction, ϵ_n are the energy eigenvalues, $\Delta(z)$ is the pair potential, and $U(z)$ is the scattering potential at each F/S interface, given by:

$$U(z) = \sum_{i=1}^{(N_L-1)/2} [U(i(d_S+d_F), z) + U((i(d_S+d_F) - d_F), z)], \tag{2}$$

where we take $U(z_l, z) \equiv H\delta(z - z_l)$, z_l is the location of the interface, H is the scattering parameter, and N_L represents the total number of layers (superconducting plus magnetic). The ferromagnetic exchange energy $h_0(z)$ takes the constant value h_0 in the F layers, and zero elsewhere. Other relevant material parameters are taken into account through the variable bandwidth $E_F(z)$. This is taken to be $E_F(z) = E_{FS}$ in the S layers, while in the F layers one has $E_F(z) = E_{FM}$ so that in these regions the up and down bandwidths are respectively $E_{F\uparrow} = E_{FM} + h_0$, and $E_{F\downarrow} = E_{FM} - h_0$. The dimensionless parameter I, defined as $I \equiv h_0/E_{FM}$, conveniently characterizes the magnets' strength. The ratio $\Lambda \equiv E_{FM}/E_{FS} \equiv (k_{FM}/k_{FS})^2$ describes the mismatch between Fermi wavevectors on the F and S sides, assuming parabolic bands with k_{FS} denoting the Fermi wave vector in the S regions. The dimensionless parameter $H_B \equiv mH/k_{FS}$ characterizes the interfacial scattering strength. We consider here singlet pairing only and, consistent with this choice, we assume that the magnetic orientation in all magnetic layers, when more than one is

present, is the same.

The nontrivial spatial dependence of the pair potential must be calculated in a self consistent manner by an appropriate sum over states:

$$\Delta(z) = \frac{\pi g(z) N(0)}{k_{FS} d} \sum_{|\epsilon_n| \leq \omega_D} \int d\varepsilon_\perp \left[u_n^\uparrow(z) v_n^\downarrow(z) + u_n^\downarrow(z) v_n^\uparrow(z) \right] \tanh(\epsilon_n / 2T), \quad (3)$$

where $N(0)$ is the density of states (DOS) per spin of the superconductor in the normal state, d is the total system size in the z direction, T is the temperature, ω_D is the cutoff "Debye" energy of the pairing interaction, and $g(z)$ is the effective coupling, which we take to be a constant g within the superconductor regions and zero elsewhere. The quasiparticle amplitudes, $u_n^\downarrow$ and $v_n^\uparrow$ involved in the sum are extracted from the solution to (1) by using symmetry arguments [30].

An appropriate choice of basis allows Eqs. (1) to be transformed into a finite $2N \times 2N$ dimensional matrix eigenvalue problem in wave vector space:

$$\begin{bmatrix} H^+ & D \\ D & H^- \end{bmatrix} \Psi_n = \epsilon_n \, \Psi_n, \quad (4)$$

where $\Psi_n^T = (u_{n1}^\uparrow, \ldots, u_{nN}^\uparrow, v_{n1}^\downarrow, \ldots, v_{nN}^\downarrow)$, are the expansion coefficients associated with the set of orthonormal basis vectors, $u_n^\uparrow(z) = \sqrt{2/d} \sum_{q=1}^N u_{nq}^\uparrow \sin(k_q z)$, and $v_n^\downarrow(z) = \sqrt{2/d} \sum_{q=1}^N v_{nq}^\downarrow \sin(k_q z)$. The longitudinal momentum index k_q is quantized via $k_q = q/\pi d$, where q is a positive integer. The label n encompasses a sum over the index q and the value of $\varepsilon_\perp$. The finite range of the pairing interaction ω_D, implies that N is finite. We have calculated the matrix elements in Eq. (4) elsewhere [9], and for brevity, the results are suppressed here.

We are mainly interested in the quantity of most experimental relevance: the local density of states (LDOS). The LDOS is related to the convolution of one-particle spectral functions for the S and F regions, and is defined as $N(z, \varepsilon) = N_\uparrow(z, \varepsilon) + N_\downarrow(z, \varepsilon)$, where the LDOS for each spin orientation is given by,

$$N_\sigma(z, \epsilon) = -\sum_n \Big\{ [u_n^\sigma(z)]^2 f'(\epsilon - \epsilon_n) + [v_n^\sigma(z)]^2 f'(\epsilon + \epsilon_n) \Big\}. \quad (5)$$

Here $\sigma = \uparrow, \downarrow$ and $f'(\epsilon) = \partial f / \partial \epsilon$ is the derivative of the Fermi function.

3 Results

In this section we present results for the LDOS and for the pair amplitude $F(\mathbf{r}) = \langle \hat{\psi}_\downarrow(\mathbf{r})\hat{\psi}_\uparrow(\mathbf{r})\rangle$, where the $\hat{\psi}_\sigma$ are the usual annihilation operators. The results are given as a function of the dimensionless parameters I, H_B and Λ, as indicated. The geometrical parameters will be given in dimensionless form in terms of the inverse of k_{FS}: $D_S \equiv k_{FS}d_S$ and $D_F \equiv k_{FS}d_F$. We take $D_F = 10$ and $d_S = \xi_0$, where ξ_0 is the BCS coherence length, with $D_S = 100$. The cutoff frequency is fixed to $\omega_D = 0.04E_{FS}$. From these values and standard relations one infers g. The temperature will be fixed to $T = 0.01T_c^0$, where T_c^0 is the bulk transition temperature of S. All results will be presented in convenient dimensionless form as indicated.

Our equations (including the self consistent condition) are numerically solved using a previously described[7,9,30,31] iteration process. The different possible self consistent states are found by starting the iteration process with initial guesses of different types. For example, for an SFS structure one can start either with a "0" or a "π" initial guess. The resulting self consistent state reached after iteration and convergence will be of the initial type, if such a self consistent state exists at least as a metastable state (a local minimum of the free energy) for the parameter values and geometry under consideration: otherwise[9] the process converges to a different configuration.

We consider three layer SFS and seven layer $SFSFSFS$ structures. In the first case, there is only one junction, and it can be in either the 0 or the π state. In the second case, there are three junctions, each of which can in principle be in a 0 or π state. Each overall junction configuration can then be characterized by specifying the three values, each zero or π, corresponding to the state of each junction.

3.1 Structures

In this subsection we present some results for the superconducting correlations in SFS and $SFSFSFS$ structures, as described by the pair amplitude, $F(z)$. We do this to illustrate the possible self-consistent pair amplitude configurations that arise as parameters such as the interface scattering strength H_B, the Fermi wavevector mismatch Λ, and the magnetic polarization strength I vary. This short discussion will establish what the different structures encountered look like, some of their stability properties, and our notation. The presentation is most clearly and efficiently illustrated by means of 3-D plots.

To begin, we display, in Fig. 1, the pair amplitude (normalized to F_0, its bulk superconductor value) for a three layer SFS system, as a function of position

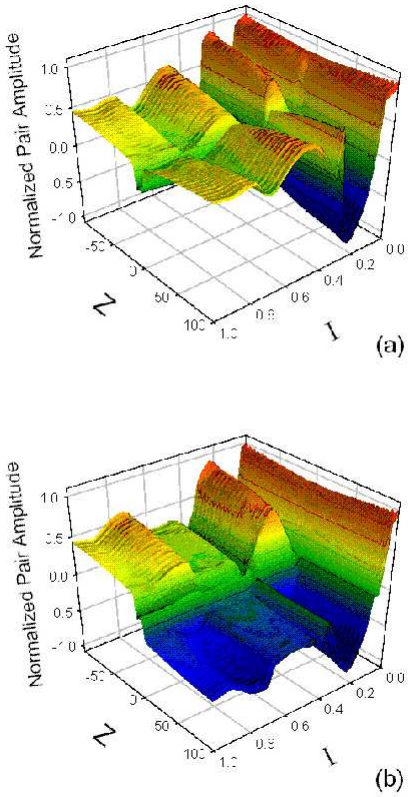

Fig. 1. The pair amplitude $F(Z)$, normalized to its bulk value F_0, for a three layer SFS structure, plotted as a function of $Z \equiv k_{FS}z$ and of the dimensionless magnetic polarization I, at $\Lambda = 1$ and $H_B = 0$. The $Z = 0$ point is at the center of the structure. Panel (a) corresponds to self consistent results obtained (see text) with an initial guess where the junction is of the "0" type and panel (b) with a "π" type. In the latter case, the solution found is of the π type except at very small I and in the neighborhood of $I \approx 0.4$, but in the former case (panel (a)), a more complicated behavior occurs, as discussed in the text.

and of the magnetic exchange parameter I in their entire ranges, without a barrier or mismatch ($\Lambda = 1$ and $H_B = 0$). The top panel shows the results of attempting to find a solution of the 0 type by starting the iteration process with an assumed piecewise constant of that form. Whether this attempt succeeds or not is reflected, of course, in the self consistent results plotted. Careful examination of the two panels reveals a rather intricate situation: one can see in the bottom panel that a solution of the π type exists nearly in the entire I range, the exception being at very small I, where the effect of magnetism becomes very weak and, as one would expect, only the 0 state solution is found. This requires small values of I, $I \lesssim 0.1$ however. One can see that near this small value, as the 0 state transitions to a π configuration, the amplitude of $F(z)$ is very small throughout the sample, which should be reflected by a sharp dip in the transition temperature. A brief instability of the π state also occurs in a small interval around $I \approx 0.4$, where the self consistent solution

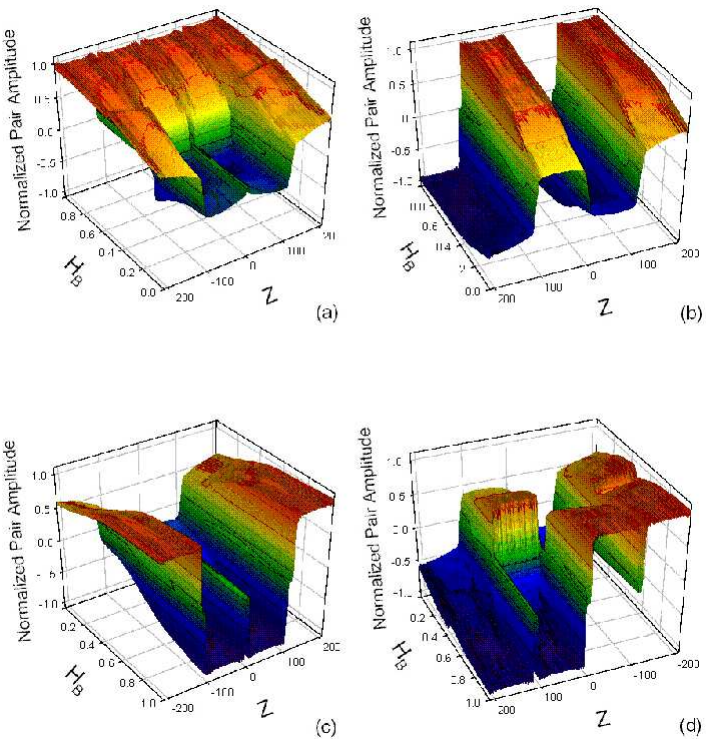

Fig. 2. The normalized pair amplitude $F(Z)$ for a $SFSFSFS$ seven layer structure, plotted as a function of Z and of the barrier height parameter H_B. Here $I = 0.2$ and $\Lambda = 1$. Panels (a) (b) (c) and (d) correspond, respectively, to attempts to find solutions of the 000, $\pi\pi\pi$, $\pi 0\pi$ and $0\pi 0$ types (see text). The resulting structure, however, it is not necessarily of the sought type, since some of the structures are unstable in part of the H_B range, as explained in the text. For clarity, the direction of increasing H_B is not the same in every panel.

is of the 0 type. This instability is reflected in Fig. 7 of Ref. [9]. On the other hand (panel (a)), one can see that there is a region of I values, $0.12 \lesssim I \lesssim 0.3$, where a 0 state does not exist. The attempt to find it fails, and the solution converges, after a very large number of iterations, to the same self consistent π state that is found, in the same I range, in panel (b).

We now illustrate the behavior of $F(z)$ in seven layer $SFSFSFS$ structures, which can be viewed as consisting of three adjacent SFS junctions. In the notation described above we denote as "000" the junction configuration when adjacent S layers always have the same sign of $\Delta(z)$, and as "$\pi\pi\pi$" when successive S layers alternate in sign. There are up to a trivial reversal, two more symmetric states: one in which $\Delta(z)$ has the same sign in the first two S layers, while in the last two it has the opposite sign, (this is labeled as the "$0\pi 0$" configuration), and the other corresponding to the two outer S layers having the same sign for $\Delta(z)$, opposite to that of the two inner S layers: these are referred to as "$\pi 0\pi$" junction configurations in our notation. We will mainly focus our study on these symmetric configurations. For the first

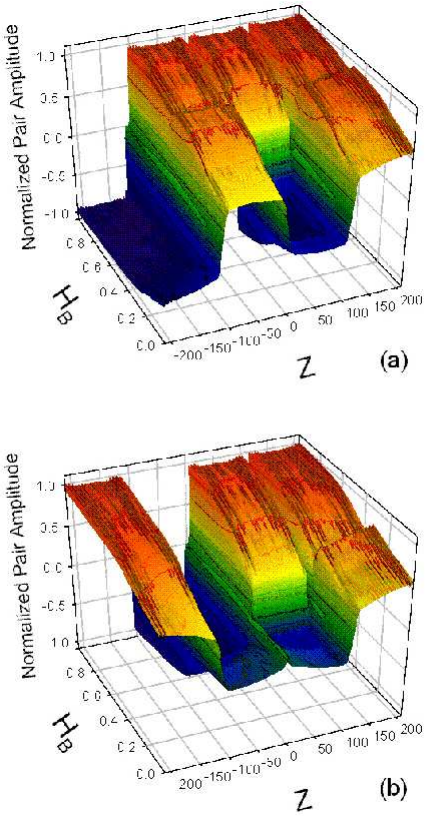

Fig. 3. The normalized pair amplitude $F(Z)$ for a $SFSFSFS$ seven layer structure, as in the previous Figure. The top and bottom panels correspond to initial attempts to find the asymmetric $\pi 00$ and $\pi\pi 0$ states respectively. Clearly such attempts only succeed when the barrier is high and the proximity effects weak (see text).

example we consider the effect of the barrier thickness, as determined by the parameter H_B. This is done in Fig. 2. In this figure we have taken $I = 0.2$ and $\Lambda = 1$ (no mismatch). The geometrical parameters and temperature are the same as in Fig. 1. The panels (a), (b), (c) and (d) correspond (in this order) to attempts to find solutions of the 000, $\pi\pi\pi$, $\pi 0\pi$, and $0\pi 0$ type. One can see that in all cases each attempt succeeds when H_B is sufficiently large, (the direction of increasing H_B has been reversed in two of the panels so that this feature is not concealed by the perspective). This makes sense, as at larger barrier heights the layers become more isolated from each other and the proximity effects must eventually become insignificant. The relative phase of $\Delta(z)$ at each S layer should then become progressively irrelevant. For the same reason, there is a clear increasing trend with increasing H_B for the absolute values of $F(Z)$ in the middle of the S layers. At smaller values of H_B, a more careful examination of the panels reveals a rather intricate situation: two of the junction configurations, $\pi\pi\pi$ and $\pi 0\pi$ (panels (b) and (c) respectively), exist in the entire range of H_B, while attempts to find a 000 structure (panel (a)) result in a $\pi 0\pi$ configuration for small barrier heights $H_B \lesssim 0.48$, and similarly, attempts to find a $0\pi 0$ structure result in a self

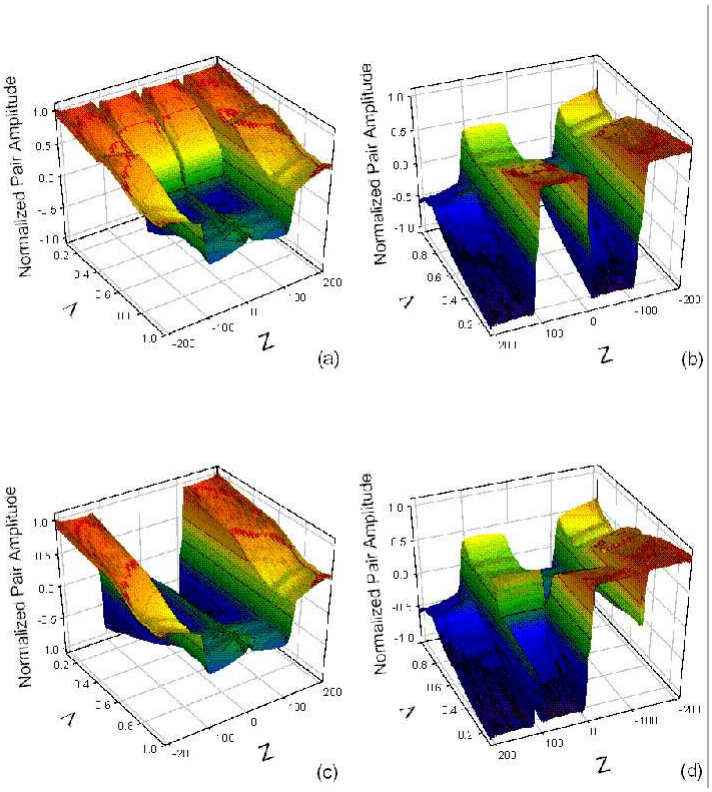

Fig. 4. The normalized pair amplitude $F(Z)$ for a $SFSFSFS$ seven layer structure, plotted as in Fig. 2 and with the same panel arrangements, but as a function of the mismatch parameter Λ at zero barrier. Note that the direction of increasing Λ is, for clarity, not the same in all the panels.

consistent $\pi\pi\pi$ configuration for $H_B \lesssim 0.44$. This is in perfect agreement with the stability analysis of Ref. [9]. Both of these "transitions" consist simply of the flipping of the two outer junctions, with the inner one remaining in the same configuration.

For completeness, we show in Fig. 3, results for the two possible asymmetric states that can exist ($\pi 00$ and $\pi\pi 0$). The parameter values are identical to the symmetric case exhibited in the previous figure. The top panel (a) corresponds to the self-consistent profile when an assumed form for the pair potential corresponds to a $\pi 00$ junction, while the bottom panel is for a $\pi\pi 0$ initial guess. It is evident that, for reasons specified above, at large enough values of the scattering parameter H_B both asymmetric states are stable self-consistent solutions. We find that the $\pi 00$ state is stable for $H_B \gtrsim 0.52$, while the $\pi\pi 0$ junction is more robust, retaining its asymmetric configuration over a larger range of H_B values, $H_B \gtrsim 0.35$. However, for weaker barriers, where the proximity effects are important, these asymmetric states are not stable, becoming $\pi\pi\pi$ and $\pi 0\pi$ respectively.

In Fig. 4 we consider the influence of the Fermi wavevector mismatch, characterized by the parameter $\Lambda \equiv E_{FM}/E_{FS}$. This figure is completely analogous

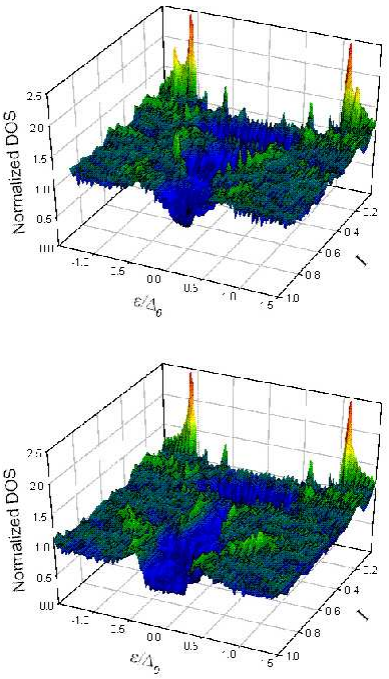

Fig. 5. The normalized DOS (see text) for a SFS trilayer, plotted as a function of the energy (in units of the bulk zero temperature gap), and of the exchange energy parameter $I \equiv h_0/E_{FS}$. The panel arrangement is the same as in Fig. 1: therefore the plots correspond to 0 and π self consistent states as in that figure.

to Fig. 2, except for the substitution of Λ for H_B, which is set to zero (no barrier). We see that for sufficiently large mismatch (small Λ), all four junction configurations exist. This is because increasing the mismatch does, in effect, isolate the superconducting regions from each other just as efficiently as increasing the barrier does. This can be roughly understood qualitatively from simple quantum mechanical considerations. For smaller mismatch, only the two solutions of the $\pi\pi\pi$ and $\pi 0\pi$ type exist: again 000 turns into $\pi 0\pi$ (for $\Lambda \gtrsim 0.48$) while $0\pi 0$ turns into $\pi\pi\pi$ at $\Lambda \gtrsim 0.57$, these results being in agreement [9] with those of detailed stability studies.

3.2 DOS

We now present some of our results for the LDOS, which is the main focus of our paper. Although the quantity $F(z)$ gives useful information regarding the superconducting correlations in the structure, it is the LDOS which is experimentally measured. The results given are in all cases for the quantity $N_\sigma(z, \epsilon)$ defined in Eq. (5), summed over σ, and integrated over a distance of one coherence length (or, equivalently, the thickness of one superconducting layer) from the edge of the sample. We normalize our results to the corresponding value for the normal state DOS of the superconducting material, and the en-

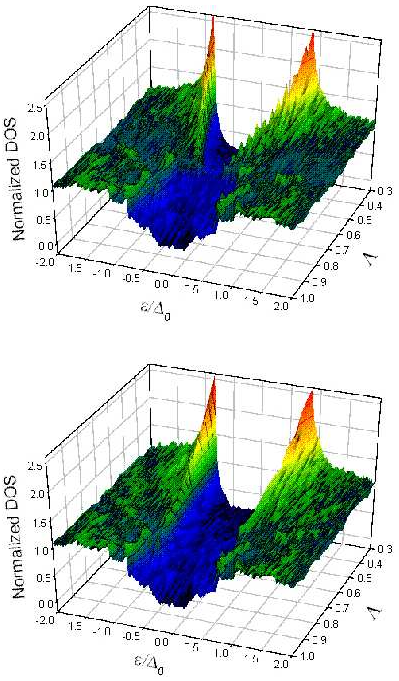

Fig. 6. The normalized DOS for a SFS trilayer, plotted as a function of the energy, and of the mismatch parameter Λ, at $I = 0.2$ and $H_B = 0$. The panel arrangement again corresponds to that in Fig. 1. In the bottom panel, the results plotted are for a self consistent π structure, while in the top panel they are for a 0 structure for $\Lambda < 0.64$ and a π structure at smaller mismatch, when the 0 structure is not stable.

ergies to the bulk value of the gap at zero temperature, Δ_0. The results shown are for the three and seven layer geometries discussed at the beginning of this section. Material parameters not otherwise mentioned are set to the "default" values of $H_B = 0$, $\Lambda = 1$ and $I = 0.2$

Figure 5 characterizes the sensitivity of the LDOS, in a SFS junction, to variations in the dimensionless exchange field parameter, I. The panel arrangement is as in Fig. 1. The top panel, therefore, shows the resultant DOS when the structure is predominately in the 0 state configuration, the exception being a small range of I as discussed in conjunction with Fig. 1, where the 0 state is unstable. The bottom panel shows the results for the π junction case, except at very small I. The limiting case of an SNS junction ($I = 0$) displays (as can be seen in either panel) subgap Andreev bound states that quickly decay as I increases. Upon varying I, the number of subgap states oscillates as a function of I, in a manner that is dependent on whether the stable state is 0 or π.

In Fig. 6 we show some other results for the same three layer system. The figure shows the normalized local density of states, as specified above, as a function of energy and mismatch Λ, at fixed $I = 0.2$. The panel arrangement is again as in Fig. 1: the bottom panel represents the results for a π configuration, while

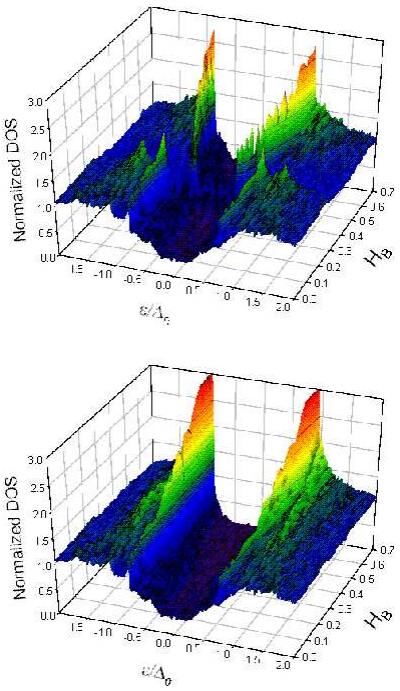

Fig. 7. The normalized DOS for a SFS trilayer, plotted and displayed as in Fig. 6, and under the same conditions, but as a function of barrier height rather than mismatch. The results shown in the bottom panel correspond to a π structure, while those the top panel they are for a 0 structure for $H_B > 0.29$ and a π structure at smaller barrier height values, when the 0 structure is not stable (see text).

the top panel shows the results for the 0 configuration at larger mismatch, $\Lambda < 0.64$, while for smaller mismatch, where the 0 configuration does not[9] exist, it repeats the results of the π configuration. The change in the results reflecting the onset of the 0 configuration instability at $\Lambda = 0.64$ can be discerned in panel (a). At larger mismatch (smaller Λ, the back portion of the figures), where both states can coexist, one can clearly see in the figure the difference between the two configurations. This is helped because in general when there is more mismatch the proximity effect weakens, the gap opens and larger peaks form which progressively become more BCS-like as the mismatch increases (Λ decreases) to $\Lambda = 0.2$. The way this occurs, too, is not the same for the 0 and the π configurations.

In the next figure, Fig. 7, we repeat the previous study but in terms of the barrier height, rather than the mismatch. Again, we plot in each panel the self consistent results obtained with initial guesses of the 0 and π types, which means that all regions of the (b) panel correspond to self consistent π states whereas those in the top panel correspond to 0 configurations, except for $H_B < 0.29$ where no self consistent 0 state exists[9]. We then plot instead results for the same π state as in the bottom panel, which is reached by iteration of either an initial 0 or π guess. Again, the point where the transition occurs can be seen as a clear discontinuity in panel (a). The difference between

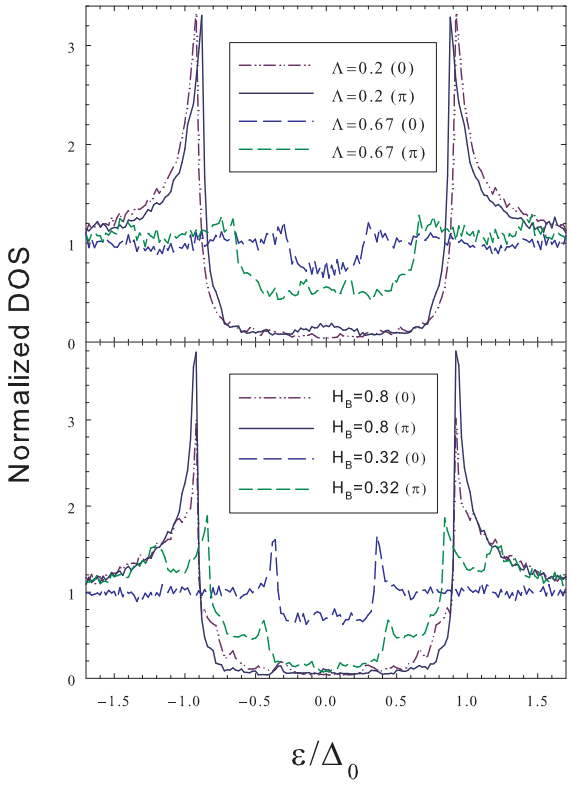

Fig. 8. The normalized DOS for a SFS trilayer, plotted as a function of the energy. Results for both 0 and π self consistent states are given, as indicated. These are slices from Figs. 6 and 7. In the top panel, the DOS is shown at $H_B = 0$ for two different values of the mismatch parameter, $\Lambda = 0.2$, and 0.67, the latter being a case for which the 0 state is nearly unstable (see text). The bottom panel shows the DOS profile in the absence of mismatch ($\Lambda = 1$), but with the interface scattering parameter H_B taking on the two values shown, chosen on similar criteria as the Λ values (see text).

the DOS for the two states where they coexist is in this case even more obvious than in the previous one, with the BCS like peaks being considerably higher for the π configuration.

It is also illustrative to display more clearly some of the features of the results by isolating some selected slices of the 3-D plots as 2-D line drawings. This we do in Fig. 8. In the top panel of this figure we present results for an SFS trilayer, for two contrasting values of the mismatch parameter Λ. Results

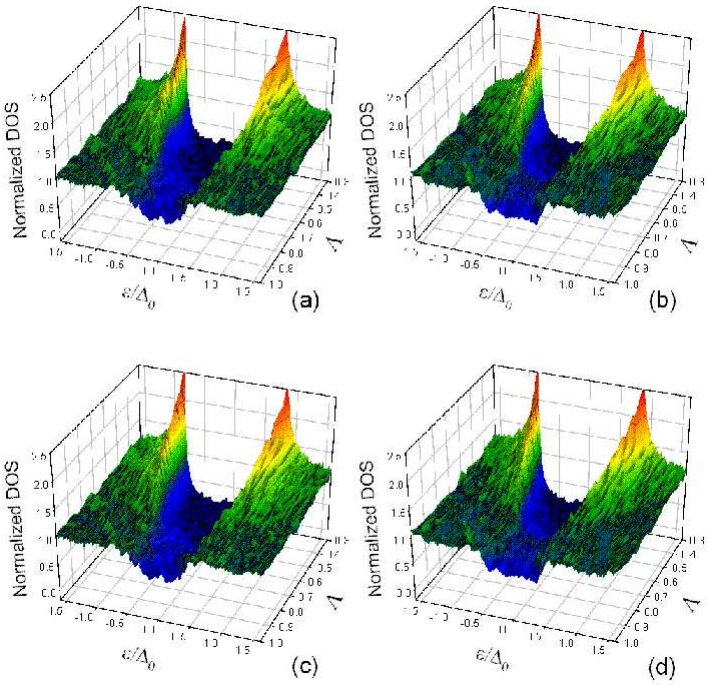

Fig. 9. The normalized DOS for the $SFSFSFS$ structure of Figs. 2 and 4, with the same panel arrangements as in those figures, plotted as a function of the energy and of the mismatch parameter Λ.

labeled as "0" and "π" are for the case where the self consistent states plotted are of these types. The 0 and π state curves corresponding to $\Lambda = 0.67$, where (as shown above and in Ref. [9]) the 0 state is barely metastable, have clearly distinct signatures, with a smaller gap opening for the 0 state, and consequently more subgap quasiparticle states. Consistent with this, when there is little mismatch one finds that the pair amplitude is relatively large in the F layer. In agreement with what was seen in Fig. 6, this progression takes a different form for the 0 and π states, and this is reflected in this panel, as can see by careful comparison of the curves. In the bottom panel we demonstrate the effect of the barrier height. The results are displayed as in the top panel, but with the dimensionless height H_B taking the place of the mismatch parameter. This figure should be viewed in conjunction with Fig. 7. One of the values of H_B chosen ($H_B = 0.32$) is again such that the 0 state is[9] barely metastable, while for the other value the 0 and π states have similar condensation energies. For H_B close to 0.32 there is a marked contrast between the two plots, with the gap clearly opening wider and containing more structure for the π state. At larger H_B the gap becomes larger in both cases, with the BCS-like peaks increasing in height. Thus, as the barrier becomes larger, one is dealing with nearly independent superconducting slabs and the plots become more similar. The largest difference therefore occurs, as for the mismatch, at the intermediate values more likely to be found experimentally.

Now we turn to the DOS results for the seven layer structure. In Fig. 9 we

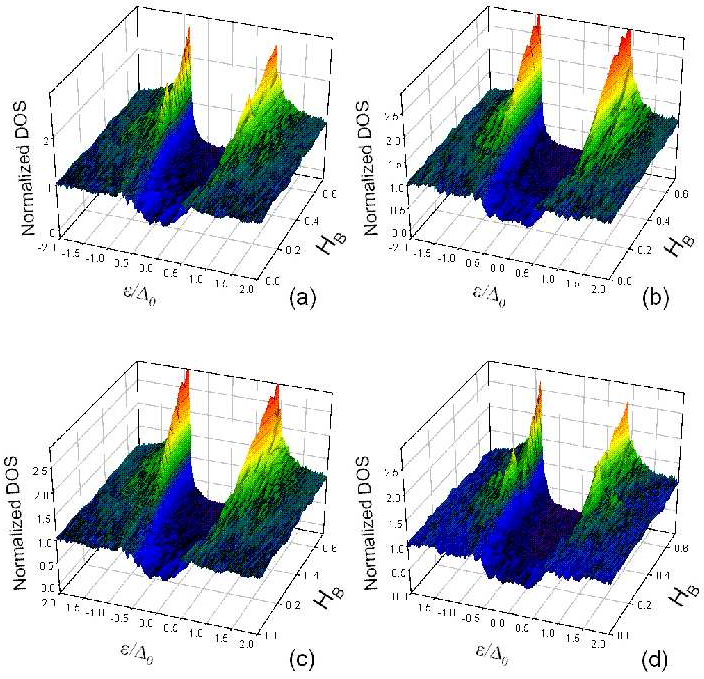

Fig. 10. The normalized DOS for the $SFSFSFS$ structure of Figs. 2, 4 and 9, plotted as in Fig. 9 except as a function of barrier height H_B instead of Λ.

present results for the normalized local DOS, defined as in the three layer case, as a function of energy and mismatch parameter. The panel arrangement in this figure corresponds to that in Fig. 4, with however a lower bound of $\Lambda = 0.3$ in the mismatch parameter, in order to better display the more intricate LDOS structure. The results shown are for the self consistent state reached by starting from each of the four symmetric junction configurations. For larger mismatch, which corresponds to the back portion of the plots, all results are therefore similar, as the LDOS reflects the independent nature of the isolated slabs (the phase is irrelevant in this limit). For small mismatch (the ranges are indicated in the discussion of Fig. 4) the results of panel (a) coincide with those of panel (c) and those of panel (d) with those of (b), as can be seen by comparing the front portions of these panel pairs. The transitions can be noted in the plots. Examination of the results shows clear differences between the four configurations. As in the three layer case, the peaks are more prominent at larger mismatch, and the "gap" is wider. At small mismatch, where only two configurations are stable, the gaps fill up and the peaks become very small for both cases, namely $\pi\pi\pi$ (panel (b) or large Λ region of panel (d)), and $\pi 0\pi$ (panel (c) or front region of panel (a)).

A similar situation occurs as a function of the barrier parameter H_B as shown in Fig. 10, which corresponds to the same conditions as Fig. 2, with the same conventions and panel arrangements. In this case, however, the BCS peaks are (at larger barrier heights) more prominent for the $\pi\pi\pi$ and $\pi 0\pi$ configurations since the S layers are not yet completely decoupled at the largest H_B shown,

which (again for clarity) is smaller than that used in Fig. 2. The peaks weaken and the gap narrows and fills up at small barrier heights, as the proximity effect strengthens. The prominence or weakening of the peaks is associated[9] with an increase or decrease of the condensation energy of the corresponding configuration, as one would intuitively expect. For small barrier heights we note also that the two states that exist in this case ($\pi\pi\pi$ and $\pi 0\pi$) have again clearly different signatures, as can be seen by comparing the front (small H_B) portions of diagrams (a) and (c) with those of (b) and (d). A similar situation occurs at small mismatch (larger Λ), in Fig. 9.

4 Conclusions

We have seen in this paper that the different junction configurations that compete in stability for different ranges of the relevant parameters, yield rather characteristic signatures in the local DOS. Thus, our results illustrate that the complex and nontrivial behavior of the pair amplitude in clean layered F/S nanostructures is reflected in the LDOS. The numerical method used here is based upon self consistent solution of the BdG equations. One advantage of this method is that it properly takes into account the atomic-scale and quantum interference effects that are likely to be important in these systems. For the SFS and $SFSFSFS$ structures investigated here, one can have up to two and six independent locally stable configurations, respectively; as the number of layers increases, so too does the number of possible configurations. Quantitatively, we have shown that the larger the scattering strength at the interfaces, or the mismatch between Fermi wavevectors of the F and S regions, the greater the number of stable states, since the proximity effects weaken. The various pair amplitude profiles however, exhibited distinct spatial forms in each case. We confirmed[7,9,33] that it is essential to calculate the pair potential self consistently, since[9] as the results shown here demonstrate, multilayer configurations can transition from one state to another abruptly, as one varies any one of the physical parameters: the magnetic exchange energy I, interface scattering strength H_B, and the Fermi wavevector mismatch Λ.

The diverse behavior observed in the pair amplitude is found to be reflected in the calculated energy spectra. When several self-consistent pair amplitude configurations coexist, each representing a local or global minimum of the free energy, they yield specific signatures in the local DOS, which are susceptible to measurement in local tunneling spectroscopy experiments. For a trilayer SFS junction, variations in the exchange field parameter I lead to oscillations in the number of subgap states, and there are similar changes in the seven layer spectrum. We also investigated the LDOS profiles by separately varying H_B and Λ. In the limiting cases of large H_B or small Λ the LDOS takes its typical BCS-like form, with few subgap quasiparticle states. The LDOS in general

however, has characteristic peaks and dips that depend on the symmetry of the ground state, and on H_B, I or Λ.

It would be of obvious interest to examine whether or not the configuration changes that occur as the material parameters are varied can happen also as a function of temperature. This question is now under investigation.

References

[1] A.K. Gupta, L. Cretinon, N. Moussy, B. Pannetier, and H. Courtois, Phys. Rev. B **69**, 104514 (2004)

[2] L. Cretinon, A. Gupta, B. Pannetier and H. Courtois, Physica C **404**, 103 (2004).

[3] A.F. Andreev, Zh. Eksp. Teor. Fiz. **46**, 1823 (1964) [Sov. Phys. JETP **19** 1228 (1964)].

[4] P. Fulde and A. Ferrell, Phys. Rev. **135**, A550 (1964).

[5] A. Larkin and Y. Ovchinnikov, Sov. Phys. JETP **20**, 762 (1965).

[6] L.N. Bulaevskii, V.V. Kuzii, and A.A. Sobyanin, Pis'ma Zh. Eksp. Teor. Fiz. **25**, 314 (1977) [JETP Lett. **25**, 290 (1977)].

[7] K. Halterman and O.T. Valls, Phys. Rev. B **69**, 014517 (2004).

[8] Y.A. Izyumov, Y.N. Proshin, and M.G. Khusainov, Phys. Usp. **45**, 109 (2002).

[9] K. Halterman and O.T. Valls, Phys. Rev. B **70**, 104516 (2004).

[10] A. Buzdin, Phys. Rev. B **62**, 11377 (2000).

[11] M. Zareyan, W. Belzig, and Y.V. Nazarov **86**, 308 (2001).

[12] K. Halterman and O.T. Valls, Physica C **397**, 151 (2003).

[13] D. Huertas-Hernando and Y.V. Nazarov, cond-mat/0404622 (unpublished).

[14] J. Koltai, J. Cserti, and C.J. Lambert, Phys. Rev. B **69**, 092506 (2004).

[15] E. Vecino, A. Martín-Rodero, and A.L. Yeyati Phys. Rev. B **64**, 184502 (2001).

[16] I. Baladié and A. Buzdin Phys. Rev. B **64**, 224514 (2001).

[17] F.S. Bergeret, A.F. Volkov, and K.B. Efetov, Phys. Rev. B **65**, 134505 (2002).

[18] A. Vedyayev, A. Buzdin, D. Gusakova, and O. Kotelnikova cond-mat/0401037 (unpublished).

[19] N. Stefanakis, R, Melin, Journ. of Phys.-Cond. Mat. **15**, 3401 (2003).

[20] Z. Faraii and M. Zareyan, Phys. Rev. B **69**, 014508 (2004).

[21] T. Luck T and U. Eckern, Journ. of Phys.-Cond. Mat. **16**, 2071 (2004).

[22] T. Kontos, M. Aprili, J. Lesuer, and X. Grison, Phys. Rev. Lett. **86**, 304 (2001).

[23] M.A. Sillanpää, T.T. Heikkila, R.K. Lindell, and P.J. Hakonen, Europhys. Lett. **56**, 590 (2001).

[24] L. Cretinon, A.K. Gupta, B. Pannetier, H. Courtois, H. Sellier, and F. Lefloch, Physica C **404**, 110 (2004).

[25] W. Guichard, M. Aprili, O. Bourgeois, T. Kontos, J. Lesueur, and P. Gandit, Phys. Rev. Lett. **90**, 167001 (2003).

[26] T. Kontos, M. Aprili, J. Lesueur, F. Genet, B. Stephanidis, and R. Boursier, Phys. Rev. Lett. **89**, 137007 (2002).

[27] V.V. Ryazanov, V.A. Oboznov, A.Y. Rusanov, A.V. Veretennikov, A.A. Golubov, and J. Aarts, Phys. Rev. Lett. **86**, 2427 (2001).

[28] S.M. Frolov, D.J. Van Harlingen, V.A. Oboznov, V.V. Bolginov, and V.V. Ryazanov, cond-mat/0402434 (2004).

[29] J. Cayssol and G. Montambeaux, cond-mat/0404215 (2004).

[30] K. Halterman and O.T. Valls, Phys. Rev. B **65**, 014509 (2002).

[31] K. Halterman and O.T. Valls, Phys. Rev. B **66**, 224516 (2002).

[32] P.G. de Gennes, *Superconductivity of Metals and Alloys* (Addison-Wesley, Reading, MA, 1989).

[33] K. Halterman and J.M Elson, J. Phys.: Condens. Matter **15**, 5837 (2003).